

The Changing Cryosphere: Pan-Arctic Snow Trends (1979-2009)

Glen E. Liston

Cooperative Institute for Research in the Atmosphere, Colorado State University, Fort Collins,
Colorado

and

Christopher A. Hiemstra

U.S. Army Cold Regions Research and Engineering Laboratory, Ft. Wainwright, Alaska

Submitted to

Journal of Climate

December 2010

Corresponding author address: Dr. Glen E. Liston, Cooperative Institute for Research in the
Atmosphere, Colorado State University, Fort Collins, CO 80523-1375 USA.

Tel: 970-491-8220; Fax: 970-491-8241; E-mail: liston@cira.colostate.edu

ABSTRACT

Arctic snow presence, absence, properties, and amount are key components of Earth's changing climate system with far-reaching physical and biological ramifications. Due to a number of measurement and modeling obstacles and scaling issues, pan-Arctic snow properties, particularly snow water equivalent depth (SWE), have been difficult to estimate at the temporal and spatial resolutions required to understand where Arctic snow covers are changing. However, recent dataset and modeling developments permit relatively high-resolution (10 km horizontal grid; 3 hourly time-step) pan-Arctic snow property estimates for 1979-2009. Using MERRA atmospheric reanalysis, land cover, and topography data, in conjunction with the MicroMet and SnowModel modeling tools, we created a dataset of distributed air temperature, snow precipitation, snow-season timing and length, maximum SWE, average snow density, snow sublimation, and rain on snow events. A dominant feature of the snow-property trends is the regional variability. Regions of positive and negative trends are distributed throughout the pan-Arctic domain, featuring, for example, spatially distinct areas of increasing and decreasing SWE or snow season length. In spite of the strong regional variability, the data clearly show a general snow decrease throughout the Arctic. Maximum winter SWE has decreased, snow onset in fall is later, the snow-free date in spring is earlier, and days with snow cover have decreased. The domain-averaged air temperature trend when snow was on the ground was $0.17\text{ }^{\circ}\text{C decade}^{-1}$ with minimum and maximum regional trends of -0.55 and $0.78\text{ }^{\circ}\text{C decade}^{-1}$, respectively. The trends for total number of snow days in a year averaged $-2.49\text{ days decade}^{-1}$ with minimum and maximum regional trends of -17.21 and $7.19\text{ days decade}^{-1}$, respectively. The average trend for peak SWE in a snow season was $-0.17\text{ cm decade}^{-1}$ with minimum and maximum regional trends of -2.50 and $5.70\text{ cm decade}^{-1}$, respectively.

1. Introduction

Ample evidence indicates the Arctic is changing. Available long-term temperature observations show warming trends of variable strength throughout the Arctic (Serreze et al. 2000; Overland et al. 2004; Chapin et al. 2005; Hinzman et al. 2005; White et al. 2007) and model simulations and future scenarios point to a warmer Arctic overall, especially with continued summer sea ice loss (Solomon et al. 2007; Holland et al. 2010). Arctic permafrost temperatures, monitored from boreholes 10-20 m deep, increased 2° C in the last 20-30 years (Romanovsky et al. 2010). The Arctic Ocean's summer sea ice extent continues to shrink and the coverage and thickness of multi-year ice is in marked decline (Serreze and Francis 2006; Stroeve et al. 2007; Gerland et al. 2008; Holland et al. 2010).

Arctic terrestrial precipitation trends are inherently more difficult to detect given cold environment snow measurement challenges with sparsely distributed observations, relatively rare long-term records, chronic station record discontinuities, variable gauge designs, low precipitation amounts, and high winds (Adam and Lettenmaier 2003; Yang et al. 2005; Bonsal and Kochtubajda 2009; Turner and Overland 2009). These factors make point observations of snow especially problematic in terms of broader representation and for identification of long-term trends, yet valiant attempts in identifying trends have been made nonetheless. New et al. (2001) reported a 0.32 cm decade⁻¹ increase in precipitation (from 1901-1998) using station data from 60 to 80 °N latitude. Hinzman et al. (2005) highlighted a handful of mostly non-significant and slight increases or decreases in long-term Arctic precipitation records; two stations with significant differences registered precipitation increases. Unfortunately, given the uncertainties and spatial variability of snow, the distribution of snow gauge observations does not lend itself to coarser-scale extrapolations of precipitation trends beyond isolated landscapes of intensive study.

More frequently, snow cover data (mostly satellite visible data) are used to identify changes in the arrival and longevity of terrestrial snow (Frei and Robinson 1999; Serreze et al. 2000; Dye 2002; Stone et al. 2002; Brown et al. 2007; Brown and Mote 2009; Zhao and Fernandes 2009; Brown et al. 2010; Choi et al. 2010). With terrestrial snow, presence or absence frequently serves as a surrogate measure of snow and cryosphere change since visible wavelengths cannot be used to estimate the amount of water present. These approaches are particularly adept at capturing changes in snow arrival, departure, and duration. Unfortunately, changes in snowmelt processes and their important energy feedback consequences (Chapin et al. 2005; Euskirchen et al. 2009), and changes from years to decades in snow water equivalent depth (SWE) distributions, are still lacking. While substantial strides are being made in SWE algorithms using passive microwave data (Armstrong and Brodzik 2001; Wulder et al. 2007; Derksen et al. 2010), uncertainties with algorithm applications, snow properties, land cover, and coarse-scale measurement issues persist, limiting the confidence and applicability of these data for trend analyses.

An alternative method of estimating Arctic snow properties (e.g., cover, SWE, duration) and their changes over time is through models. General circulation models (GCMs) have been used to address Arctic climate change and precipitation questions for past and future conditions (Räisänen 2008; Walsh et al. 2008; Finnis et al. 2009b; Finnis et al. 2009a); these studies generally find higher temperatures lead to increases in Arctic precipitation. Efforts have been made to link land surface hydrology models to reanalyses or GCM data to specifically address Arctic (Pohl et al. 2007; Slater et al. 2007) or relatively high resolution (0.5 degrees) global (Adam et al. 2009) snow processes.

Inasmuch as these coarse-scale modeling approaches can answer critical physical

questions, one substantial deficiency is their resolution. In most cases, the scales at which GCMs and these other models operate (0.5 to 2.5 degrees; Shukla et al. 2010) are too coarse to capture key snow processes, heterogeneities, and land-cover and snow interactions (Liston 2004). Modeling capabilities have grown, along with improvements in computing power and the emergence of relatively high-resolution topographic, land cover, and meteorological data products. Together, these tools and datasets can be combined to provide a reasonable facsimile of cryospheric processes and allow improved understanding of the specific implications of climate change related to snow, and this can be done at much higher resolution than previously possible.

The purpose of this paper is to perform and analyze the spatial and temporal evolution of snow, snow processes, and snow characteristics in high northern latitudes, at the highest possible spatial and temporal resolution; all in an effort to understand regional spatial and temporal variations in key climate-relevant snow-related features. This is accomplished by driving a local-to regional-scale meteorological and snow-evolution modeling system with 3-hourly, $2/3^\circ$ longitude by $1/2^\circ$ latitude gridded atmospheric reanalysis datasets. The resulting snow-related modeling and analysis datasets span 30 years (1 August 1979 through 31 July 2009), covering a pan-Arctic domain with a 10-km grid increment and 3-hourly time step.

2. Model description

a. SnowModel

To quantify spatial and temporal variations in Arctic-system snow properties and characteristics, we performed model simulations using SnowModel (Liston and Elder 2006a), a spatially-distributed snow-evolution modeling system designed for application in all landscapes, climates, and conditions where snow occurs. It is an aggregation of four sub-models: EnBal

(Liston 1995; Liston et al. 1999) calculates surface energy exchanges and snowmelt; SnowPack (Liston and Hall 1995; Liston and Mernild 2010) simulates snow depth and water-equivalent evolution; SnowTran-3D (Liston and Sturm 1998; Liston et al. 2007) accounts for snow redistribution by wind; and SnowAssim (Liston and Hiemstra 2008) is available to assimilate field and remote sensing datasets. SnowTran-3D and SnowAssim were not used in these simulations.

SnowModel is designed to run on grid increments of 1- to 200-m and temporal increments of 10-minutes to 1-day. It can be applied using much larger grid increments (up to 10s of km) if the inherent loss in high-resolution (subgrid) information (Liston 2004) is acceptable. Processes simulated by SnowModel include snow precipitation; blowing-snow redistribution and sublimation; interception, unloading, and sublimation within forest canopies; snow-density evolution; and snowpack ripening and melt. SnowModel incorporates first-order physics required to simulate snow evolution within each of the global snow classes (i.e., ice, tundra, taiga, warm forest [or alpine], prairie, maritime, and ephemeral) defined by Sturm et al. (1995) and Liston and Sturm (2010). An attractive feature of the distributed SnowModel snow-evolution modeling system is its realism in physical processes and spatial and temporal distributions; it can drift snow at high elevations while simultaneously melting valley snow within the same domain. Required SnowModel inputs include temporally-variant precipitation, wind speed and direction, air temperature, and relative humidity obtained from meteorological stations and/or an atmospheric model located within or near the simulation domain. Spatially-distributed, time-invariant topography and land cover are also necessary.

b. MicroMet

Meteorological forcings required by SnowModel are provided by MicroMet (Liston and Elder 2006b), a quasi-physically-based, high-resolution (e.g., 1-m to 10-km horizontal grid increment), meteorological distribution model. MicroMet is a data assimilation and interpolation model that utilizes meteorological station datasets and/or gridded atmospheric model or (re)analyses datasets. MicroMet minimally requires near-surface air temperature, relative humidity, wind speed and direction, and precipitation data. The model uses known relationships among meteorological variables and the surrounding landscape (primarily topography) to distribute those variables over any given landscape in physically plausible and computationally efficient ways. MicroMet performs two kinds of adjustments to the meteorological data; 1) all available data fields, at a given time, are spatially interpolated over the domain, and 2) physically based sub-models are applied to each MicroMet variable to quantify topographic, elevation, and vegetation effects at any given point in space and time. Station interpolations (horizontal) to a regular grid are done using a Barnes objective analysis scheme (Barnes 1964, 1973; Koch et al. 1983). The Barnes scheme applies a Gaussian distance-dependent weighting function, where the weight that a station contributes to the value of the grid point decreases with increasing distance from the observation. Interpolation weights are objectively determined as a function of data spacing and distribution. At each time step, MicroMet distributes air temperature, relative humidity, wind speed, wind direction, incoming solar radiation, incoming longwave radiation, surface pressure, and precipitation, and makes them accessible to SnowModel.

MicroMet and SnowModel constitute a physically-based modeling system that creates value added snow information (e.g., snow depth, snow density, snow melt rate, snow thermal properties, snow cover duration, sublimation) from basic meteorological variables (e.g., air temperature, humidity, precipitation, wind). The products yielded are based on our physical

understanding of snow-evolution processes and features and their interactions with the atmosphere and surrounding land surface.

MicroMet and SnowModel have been used to distribute observed and modeled meteorological variables and evolve snow distributions over complex terrain in Colorado, Wyoming, Idaho, Oregon, Alaska, Arctic Canada, Siberia, Japan, Tibet, Chile, Germany, Austria, Svalbard, Norway, Greenland, and Antarctica as part of a wide variety of terrestrial modeling studies (e.g., Liston and Sturm 1998, 2002; Greene et al. 1999; Liston et al. 2000, 2002, 2007, 2008; Prasad et al. 2001; Hiemstra et al. 2002, 2006; Hasholt et al. 2003; Bruland et al. 2004; Liston and Winther 2005; Mernild et al. 2006, 2008, 2009, 2010; Liston and Hiemstra 2008, 2010; Liston and Mernild 2010; Mernild and Liston 2010).

3. Model simulation

a. Model configuration and simulation domain

Snow evolution and surface energy fluxes were simulated using MicroMet and SnowModel for the 30-year period from 1 August 1979 through 31 July 2009. The simulation covered a 7250-km by 7250-km domain centered on the North Pole (Fig. 1). This domain encompasses the majority of the Arctic system, defined to be the northern region of Earth where energy and moisture interact with middle latitudes (Roberts et al. 2010). The simulation domain incorporates many of the common definitions of the terrestrial Arctic system: the land surface north of the Arctic Circle; the majority of land north of the 10 °C July air temperature isotherm and the annual-average 0 °C air temperature isotherm that circle the North Pole; and the southern boundary of land draining into the northern high-latitude oceans (the simulation domain does not quite reach this in a couple locations). The model simulation was performed using a 10-km

horizontal grid increment (525,625 grid cells) and 3-hour time step. Because blowing snow does not typically move across 10-km grid cells into adjacent cells, SnowTran-3D and the associated snow-transport processes were not included in the simulation.

Topographic data used in the model simulation were obtained from NOAA's GLOBE Project (<http://www.ngdc.noaa.gov/mgg/topo/gltiles.html>), which provided 1-km digital elevation model (DEM) data that were resampled to 10 km. The land cover distribution used in the simulation was a hybrid dataset created primarily from 300 m Global Land Cover (GlobCover; <http://ionia1.esrin.esa.int/>) data augmented with the Circumpolar Arctic Vegetation Map (CAVM Team 2003). The CAVM was utilized to correct GlobCover's misclassified snow/ice (areas that should have been barren or rock) at extremely high northern latitudes ($>82^\circ$) in northern Canada and Greenland. The resulting hybrid dataset was resampled to 10 km and reclassified into SnowModel land cover classes (Liston and Elder 2006a).

Topography of the study area ranges from sea level to over 5000 meters, and land cover includes bare, wetlands, tundra, shrubs, deciduous and coniferous trees, glaciers, and ice sheets (Fig 1). Air temperatures over the entire domain are typically well below 0°C for much of the fall, winter, and spring months, and the northernmost regions spend considerable time in darkness during winter. Near-surface temperature inversions are common throughout the snow-covered Arctic (e.g., Mernild and Liston 2010). The associated thermal stability inhibits vertical mixing and produces variable local and regional climates. This, in combination with local and regional terrain influences, can produce local and regional meteorological and snow conditions that are much more elaborate than coarse-scale patterns (e.g., Lynch et al., 2001; Liston and Sturm 2002; Taras et al. 2002). The fall, winter, and spring snow seasons in this domain can range from less than 30 days to over 300 days each year. On average, each year the simulation

domain has 215 days with snow on the ground. Snow can begin accumulating as early as 1 September, and it can be 1 July before it melts completely.

b. Meteorological forcing

Atmospheric forcing data were provided by NASA Modern Era Retrospective-Analysis for Research and Applications (MERRA) products (Bosilovich 2008). This reanalysis program has the specific goal of improving water cycle processes and features while taking advantage of modern satellite era datasets. MERRA covers the period 1979-present, on a $2/3^\circ$ longitude by $1/2^\circ$ latitude global grid. Surface atmospheric forcing variables are available hourly. The analysis assimilates a wide range of satellite observations in addition to more conventional radiosonde, dropsonde, aircraft, and surface observations. Bosilovich et al. (2008) analyzed precipitation outputs from an early version of the MERRA reanalysis system, and concluded the MERRA precipitation fields were an improvement over the previous generations of reanalyses.

In preparation for the model simulation, hourly MERRA 10-m air temperature, specific humidity, surface pressure, precipitation, u and v wind component variables were aggregated to 3-hourly values. MicroMet then used these to create the 3-hourly, 10-km atmospheric forcing distributions required by SnowModel (air temperature, relative humidity, wind speed and direction, precipitation, and incoming solar and longwave radiation). The 10-km atmospheric fields were ingested by SnowModel to simulate the time evolution and spatial distribution of water and energy fluxes and states. Simulated variables included: surface (skin) temperature, albedo, outgoing longwave radiation, latent heat flux, sensible heat flux, liquid precipitation, solid precipitation, snowmelt, sublimation, snowmelt runoff, snow depth, snow density, and snow water equivalent. In addition, we generated secondary products such as the timing and

distribution of rain-on-snow events, changes in snow and growing season lengths, hydrologic budgets, winter soil microbial activity, changes in snow thermal characteristics, and changes in surface energy exchanges.

4. Model results

The 3-hourly simulated atmospheric and snow data were aggregated (averaged or summed, depending on the variable) to daily values over the 30-year simulation period for spatial and trend analyses. In addition, for each year, averages (of variables like air temperature), sums (of variables like solid precipitation), snow-onset and snow-free dates, maximum snow-water-equivalent depth during the snow year, and other secondary variables were calculated. In these calculations a 'snow' year was assumed to be 1 August through 31 July. Because of the focus here on land-based seasonal snow evolution, any grid cells containing glaciers, ice sheets, and oceans were removed from the calculations and analyses.

The 30-year average, 10-m air temperature for days with snow on the ground, is shown in Fig. 2a. The linear trends in annual averages for each grid cell are provided in Fig. 2b. The spatial variability in linear trends across this Arctic-system domain is considerable, with variations in magnitude and changes in sign occurring over distances of a few hundred km. As examples of positive (increasing with time) and negative (decreasing with time) temperature trends, annual values averaged over 250-km by 250-km regions in Alaska and Canada are presented in Figs. 2c and 2d, respectively, along with the associated linear trend lines.

The domain-average trend for air temperature with snow on the ground was $0.17\text{ }^{\circ}\text{C decade}^{-1}$ (Table 1). In addition, by defining a region to be a 250-km by 250-km area that was free of ice or ocean grid cells [such as the boxes in Fig. 2, panels (a) and (b)], minimum ($-0.55\text{ }^{\circ}\text{C}$

decade⁻¹) and maximum (0.78 °C decade⁻¹) regional trends over the simulation domain, and corresponding to minimum and maximum colors and patterns shown in Fig. 2b, were calculated (Table 1). Positive trends of this variable covered 73% of the simulation domain (Table 1). At the coarsest scale, the overall domain-averaged temperature trend was small since it was comprised of larger-magnitude temperature shifts in contrasting directions occurring across the Arctic system. Also note that because the snow-covered season changed throughout the simulation, the time period over which the temperature averaging occurred also varied from one year to the next. The domain-average air temperature trend, with and without snow on the ground (i.e., including the snow-free season) was 0.38 °C decade⁻¹, and positive trends covered 99% of the domain (Table 1).

In addition to air temperature, precipitation is a key climate-system variable. Figure 3a displays the 30-year average annual solid precipitation for each grid cell. The areas with dry, continental climates typically have annual water-equivalent precipitation totals of 10 to 30 cm, while maritime, coastal climates can have annual solid precipitation amounts in excess of 75 cm. The linear trends in solid precipitation are plotted in Fig. 3b. Again, considerable spatial variability, and both positive and negative trends are found (Fig. 3c and d). When averaged over the simulation domain, the solid precipitation linear trend almost goes to zero (-0.02 cm decade⁻¹), while the region minimum (-3.03) and maximum (8.00) are of considerably greater magnitudes (Table 1). Negative solid precipitation trends covered 64% of the domain (Table 1).

Given the important role snow cover plays in the Arctic surface energy budget and other aspects of the Arctic climate system (e.g., Serreze and Barry 2005; McGuire et al. 2006; Euskirchen et al. 2007), quantifying changes and variations in snow-cover duration, timing, and spatial patterns is essential for a comprehensive understanding of high-latitude climate changes.

The core snow season was defined to be the longest period (in days) with snow cover for each year, for each grid cell (Fig. 4a, inset). Using the model datasets and this definition, the core season snow-onset date (typically in the fall, but could be in winter), core snow-free date (typically in the spring, but could be winter or summer), length of core snow season, date of first snow accumulation (snow that lasted at least 24 hours), date of last snow on the ground, and total number of days with snow on the ground were calculated. Over the 30-year period, this domain averaged 215 days with snow on the ground, 212 days of which were during the core snow season (Fig. 4a). The distribution of 30-year linear trends are shown in Fig. 4b, c, and d. Throughout much of the Arctic there was a decrease in the snow cover duration, with a regional peak of -17.0 days decade⁻¹ (negative trends covered 75% of the domain) and a domain average of -2.6 days decade⁻¹, but there were also regions of increased snow duration, with a maximum of 8.1 days decade⁻¹ (Table 1). The trends in total number of days with snow on the ground (both the red and blue periods show in Fig. 4a, inset) were similar to those of the core snow period (Table 1). The Alaska region shown in Fig. 4c had an approximately 15-day snow cover decrease over the 30-year period. Trends in snow cover duration are strongly controlled by the combination of snow precipitation inputs (Fig. 3), and air-temperature (Fig. 2) and solar-radiation related ablation processes.

The snow-onset date in the fall (Fig. 5a) typically occurred later in the year over the 30-year period (Fig. 5b), with a domain average of 1.3 days decade⁻¹ (Table 1). Regional extremes occurred that ranged from a decrease of 10.8 days decade⁻¹ and an increase of 14.1 days decade⁻¹ (Table 1). Positive trends (snow onset later in the year) of this variable covered 65% of the domain (Table 1). The snow-free date in the spring (Fig. 6a) typically had a trend toward occurring earlier in the year (Fig. 6b), with a domain average of -1.3 days decade⁻¹ (Table 1).

Again, regional extremes ranged from -9.9 to 3.7 days decade⁻¹, with negative trends covering 80% of the domain (Fig. 6c, d; Table 1).

From a regional hydrologic perspective, moisture contained within the winter snowpack represents water storage that is made available to the climate system as a liquid when it melts in the spring. Throughout the Arctic, this spring melt is typically the largest single hydrologic event of the year, leading to a snowmelt discharge hydrograph that contains as much as 80% of the total annual runoff from many Arctic drainage basins (e.g., McNamara et al. 1998; Yang et al. 2003, 2004). This moisture storage is captured by the peak SWE during the snow season (Fig. 7a). Trends in this variable (Fig. 7b, c, d) are associated with the corresponding trends in snow precipitation (Fig. 3b, c, d). Negative trends in peak SWE covered 61% of the simulation domain (Table 1).

Snow density is a function of snow temperature (and thus air temperature and surface energy budget), temperature at which new snow falls, wind speed (breaking up snow particles), compaction (due to snow overburden), and temperature and vapor-pressure gradients within the snowpack (e.g., Liston et al. 2007). Changes in snow density represent an integrated measure of the "snow climate" the snowpack evolves within. Because of the relatively large grid-cell increment used in this model simulation, blowing snow processes were not included in the simulations (in the natural system, wind-transported snow particles are typically either captured in a topographic drift trap, captured in vegetation protruding above the snow surface, or they sublimate away completely before they travel 10 km). As a consequence, we estimate snow density values simulated by the model (Fig. 8a) in the non-forested areas of the simulation domain (Fig. 1b) are approximately 50 kg m⁻³ lower than those found in nature (Sturm et al. 2010). The snow density trends (Fig. 8b, c, d) averaged over the domain are slightly positive

(Table 1), while regional trends had minimums and maximums as large as -21.0 and $15.4 \text{ kg m}^{-3} \text{ decade}^{-1}$, respectively (Table 1).

Total snow-season sublimation is presented in Fig. 9. In the natural system, sublimation can occur from the static snow surface and from blowing snow particles. Static-surface sublimation of snow on the ground depends on air temperature, the air's moisture deficit, wind speed, and the other components of the surface energy budget. Because this simulation did not include blowing-snow processes, sublimation of wind-transported snow particles are not part of these totals; we expect non-forested area sublimation totals presented here are underestimated. In previous studies, snow sublimation has been found to be an important component of the Arctic moisture budget, representing between 10 and 50% of the total winter precipitation, and blowing-snow sublimation can be a key component of that budget (e.g., Liston and Sturm 1998, 2002, 2004). Sublimation trends (Fig. 9b, c, d; Table 1) show considerable spatial variability, with 77% of the domain having negative trends.

Rain-on-snow (ROS) events can have considerable consequences for animals living in snow-covered areas. Following Rennert et al. (2009), ROS events were defined as a minimum of 3 mm of liquid precipitation falling on a minimum of 5 mm of snow water equivalent depth (Fig. 10a). The spatial variation of ROS trends across the Arctic system domain is considerable (Fig. 10b, c, d).

5. Discussion

As a whole, the domain-averaged temperature trend was $0.17 \text{ }^\circ\text{C decade}^{-1}$; 73% and 27% of the domain showed a positive or negative trend, respectively (Table 1). Since our model simulations were performed at a relatively high resolution, marked differences in domain

elevation and land-cover patterns increased the spatial heterogeneity compared with coarser-resolution simulations. As described elsewhere (Turner and Overland 2009), the temperature change trend pattern is expected to be heterogeneous with some regions cooling and others warming over the same time period.

The largest negative temperature trends are in Yamalo-Nenets and Khanty-Mansi in the Russian Federation; Russian Amur and Northeast China; Kamchatka Russian Federation; Southwest Alaska; and the northern Canadian Archipelago (Fig. 2). The largest warming trends were in Scandinavia; vast areas of Northwest Territories, Nunavut, and Quebec, Canada; and Greenland. The pan-Arctic climate record air temperature anomaly patterns identified by Overland et al. (2004) for the coincident 1979-2002 record appear in Fig. 2, showing fidelity with meteorological station forcing data within the MERRA dataset. Likewise, 1991-2005 temperature difference patterns reported for Canada's Mackenzie River Delta (Bonsal and Kochtubajda 2009) are in general agreement with our SnowModel results. Further, the 1979-2009 0.3 °C decline in temperature associated with the Alaska Box (Fig. 2c) is corroborated with an identical observed winter temperature decline from 1977-2005 (Shulski and Wendler 2007).

Snow precipitation is distributed largely as expected (Fig. 3; Fig. 7); higher elevations and coastal ranges adjacent to warmer ocean waters have increased precipitation while interior continental regions and much of the Arctic Ocean margins are drier. The annual snow precipitation patterns appear superficially similar (considering vast scale differences) to 1979-93 ERA-40 data (Serreze et al. 2005). Pan-Arctic domain-averaged snow precipitation decreases slightly $-0.02 \text{ cm decade}^{-1}$ (Table 1), which contrasts with the 1979-1995 $\sim 0.3 \text{ cm decade}^{-1}$ increase in fall, winter, and spring precipitation (55 °N to 85 °N) reported by Serreze et al. (2000) and the $\sim 0.3 \text{ cm decade}^{-1}$ annual precipitation increase for (60 °N to 80 °N) during 1979-

1998 reported by New et al. (2001). In terms of specific sites with long-term records, Hinzman et al. (2005) reported annual precipitation trends for Barrow, Alaska ($-1.29 \text{ cm decade}^{-1}$); Fairbanks, Alaska ($0.14 \text{ cm decade}^{-1}$); Fort McMurray, Canada ($2.60 \text{ cm decade}^{-1}$); Alert, Canada ($0.12 \text{ cm decade}^{-1}$); Yakutsk, Russia ($0.50 \text{ cm decade}^{-1}$); and Tiksi, Russia ($0.06 \text{ cm decade}^{-1}$). The only significant trends were associated with Yakutsk and Fort McMurray records. With the exceptions of Fairbanks and Fort McMurray, these general trends were visible in the SnowModel simulation (Fig. 3). A later examination of Fairbanks' annual precipitation record from 1916-2006 showed a non-significant trend of $-0.54 \text{ cm decade}^{-1}$ with the strongest declines occurring with winter and spring precipitation (Wendler and Shulski 2009). The negative Fairbanks trend more closely resembles SnowModel's $-1.33 \text{ cm decade}^{-1}$ winter precipitation estimate for the Fairbanks-area (central Alaska) regional box (Fig. 3c).

The driving dataset and the associated reanalysis system (MERRA in our case) strongly influences SnowModel's simulated values and biases (Adam and Lettenmaier 2003; Yang et al. 2005; Drobot et al. 2006; Walsh et al. 2008). Clein et al. (2007) and McGuire et al. (2008) observed that different sources of reanalysis or GCM data can be highly variable, especially with episodic variables such as precipitation (as opposed to the smaller magnitude differences associated with continuous fields such as temperature).

Many have demonstrated that Arctic and Northern Hemisphere snow duration is shorter than in the past (Frei and Robinson 1999; Brown 2000; Serreze et al. 2000; Dye 2002; Brown et al. 2007; Turner et al. 2007; Brown and Mote 2009; Brown et al. 2010; McCabe and Wolock 2010; Choi et al. 2010), and SnowModel results offer additional confirmation of this trend at a higher resolution (Fig. 4). Averaged over the simulation domain, snow arrives $1.29 \text{ days decade}^{-1}$ later in fall (Fig. 5; Table 1) and departs $1.28 \text{ days decade}^{-1}$ earlier in the spring (Fig. 6; Table 1),

with the exception of coastal high-elevation mountain systems where already deep snows are getting deeper (Fig. 7). Areas with a normally shallow snow cover have briefer snow-covered periods (e.g., Alaska's North Slope) while deeper snow areas are being enhanced and have a longer snow-covered season (Fig. 4; Räisänen 2008). Our distributed snow-onset and snow-free estimates (Figs. 5-6) are largely comparable with Dye's (2002) 1972-2000 calculated trends of 0.4 to 3.6 day decade⁻¹ later fall snow arrival and -3.2 to -5 day decade⁻¹ earlier snow-free spring conditions. Spatially, SnowModel snow cover duration (Fig. 4) duplicates remote sensing analyses for Canada (Brown et al. 2007) and much coarser-resolution GCM simulation and NOAA data (Brown and Mote 2009). Further, SnowModel data show a remarkable spatial agreement with coincident (1972-2008) NOAA weekly snow cover data trends (Brown et al. 2010) with one notable exception. The NOAA dataset shows western North America coastal snow having a declining trend while SnowModel's trend is lengthened (Figs. 4-6), but other trends are largely duplicated. Snow cover duration is important for a number of reasons. Altered snow regimes can produce substantial differences in surface energy balance reflected in air temperature records, especially in spring when solar radiation is more intense (Chapin et al. 2005).

Tracking snow density changes through time (Fig. 8) and estimates of sublimation (Fig. 9) are novel contributions of this modeling effort. Density values are not normally reported in most modeling studies, although efforts are being made to describe functional snow density classes using observations (Sturm et al. 2010). Sublimation changes through time could have important ramifications for water budgets, as sublimation values are likely changing (Fig. 9) alongside precipitation amounts (Fig. 3).

Numerous studies have suggested the number of ROS events (Fig. 10) will increase under

a warming climate (e.g., Putkonen and Roe 2003; Rennert et al. 2009). Extensive winter mortality in reindeer, caribou, and muskoxen populations can result from ice-crust formation that prevents access to winter food. For example, in October 2003 an extreme ROS event killed approximately 20,000 muskoxen on Banks Island in western Arctic Canada (Putkonen et al. 2009). As another dramatic example, on Svalbard, Norway during winter 1993/1994, rain, followed by below-freezing temperatures, produced a 10-cm thick ice-crust that led to a 78% decrease in the reindeer population (360 individuals in 1993 to 78 individuals in 1994) (Aanes et al. 2000).

To help understand the physics behind our model results, and as part of our model output data analyses, we performed numerous regressions among the model output variables. The only clear relationship was between solid (snow) precipitation and peak SWE. All other attempts at finding simple relationships among basic atmospheric variables and the more complex snow-property variables (e.g., between air temperature and snow-free date) failed. We concluded that reproducing the complexity of the natural system requires physically-based modeling systems capable of accounting for the threshold and other non-linear aspects of the interactions between snow and its surrounding environment.

This model simulation is not without its limitations. The SnowModel snow evolution simulation assumed one-way atmospheric forcing, where the atmospheric conditions were prescribed at each time step without regard for the snow conditions (or lack of snow conditions) at the ground surface. In the natural system, atmospheric variables like air temperature and humidity would be modified depending on the surface state, such as snow-covered or snow-free conditions, a dry or melting snowpack, and/or protruding or buried vegetation. These feedbacks were not included in the simulation presented herein. These kinds of interactions are included in

regional and global climate models, and 30-year simulations with these models at 10-km resolution are expected to be possible in the near future (Bromwich et al. 2010; Hines et al. 2010; Shukla et al. 2010). In addition, MicroMet was used to downscale the MERRA atmospheric forcing data from its $2/3^\circ$ longitude by $1/2^\circ$ latitude grid to the 10-km SnowModel simulation grid. An atmospheric model with more physics and dynamics (a regional or global climate model) would be expected to create improved downscaled temperature and precipitation fields. Again, simulations with such a modeling system are expected to soon be possible (e.g., Bromwich et al. 2010; Hines et al. 2010). Also, as noted previously, because of the relatively large grid increment this simulation did not include blowing snow processes. This influences the simulated snow depth, snow density, SWE, sublimation distributions, and other associated aspects of the snow-cover evolution physics in all non-forested areas of the domain (Fig. 1). A solution to this limitation would be to implement a subgrid blowing snow parameterization to account for the relevant processes and interactions (e.g., Bowling et al. 2004).

6. Conclusions

High temporal and spatial resolution snow data represent a critical deficiency in current Arctic monitoring and modeling efforts. The SnowModel pan-Arctic simulation dataset offers a rich look at snow climatology and properties from 1979-2009 at unprecedented spatial (i.e., 10-km) and temporal (i.e., 3-hourly) resolution. The data were realistically distributed in time and space, and air temperature and snow onset and departure trends largely concur with previous lower resolution climate studies. The merging of state-of-the-art atmospheric forcing datasets (i.e., MERRA) with relatively high-resolution modeling tools (i.e., MicroMet and SnowModel) allowed a detailed

mapping of spatial variations in pan-Arctic snow trends. These trends exhibit strong regional variations, which are attributed to a combination of spatial variations in atmospheric forcing (primarily air temperature and solid precipitation) and spatial variations in snow-evolution physics. The non-linear interactions among snow accumulation and ablation processes created heterogeneity far beyond that seen in the basic atmospheric forcing variables (cf. Figs. 2a and 3a with 7a). MicroMet and SnowModel can be thought of as detailed process models that take our understanding of snow physics and dynamics and converts basic meteorology such as air temperature, humidity, precipitation, wind, and radiation, into the evolution of complex snow variables such as depth, density, and sublimation.

The relatively high spatial resolution of this dataset allows important insights into the regional distributions of snow-related features. A ubiquitous characteristic of the simulated snow fields is strong regional variability. Throughout the Arctic, regions of positive and negative trends are the rule rather than the exception. Positive snow-season air temperature trends covered 73% of the simulation domain, negative solid precipitation trends covered 64% of the domain, the number of days with snow on the ground decreased for over 75% of the domain, the snow-onset date was later in the year for 65% of the area, the snow-free date was earlier for 80% of the domain, and the maximum SWE decreased for over 61% of the simulation domain.

Almost without exception, the domain-averaged 30-year trends indicate decreasing snow throughout the Arctic: The number of days in the core snow season and the total number of days with snow cover has decreased over the last 30 years. The onset of snow in the fall occurs later in the year, and the snow-free date occurs earlier. The

maximum SWE found during the snow season is decreasing, the average snow density is increasing, and the number of rain on snow events is increasing. All of these are associated with increasing Arctic snow-season temperatures.

This work and its resultant datasets have implications for future avenues of investigation of snow-climate interactions. Snow has a clear influence on ground temperatures and permafrost (Bartlett et al. 2005; Zhang 2005) that can be better quantified with the SnowModel dataset. Given the importance of snow and cryospheric processes on ecosystem structure and function (Chapin et al. 2005; Clein et al. 2007; Euskirchen et al. 2007; Post et al. 2009), this snow-properties dataset represents another leap forward toward a more explicit understanding of links among snow, landscapes, and climate change. For example, snow distribution patterns and snow-free duration may well be associated with observed changes in tundra normalized difference vegetation index (NDVI) or phenology (Bunn and Goetz 2006; Verbyla 2008; Bhatt et al. 2010; de Beurs and Henebry 2010). In addition, it is likely that soil temperatures and microbial processes are also changing in light of the altered Arctic snow regime.

With a duration averaging 215 days per year, the pan-Arctic snow cover influences numerous climate-related interactions among the atmosphere, hydrosphere, biosphere, and other aspects of the cryosphere. Our current understanding and model-based representations of these interactions still suffer weaknesses associated with spatial resolution, lack of interactive physics and dynamics, inadequate observational datasets, and incomplete insight into the critical linkages and feedbacks among key processes. Future research efforts will fill these gaps and improve our understanding of the role snow plays throughout the Arctic. This model simulation and its associated analyses contributes to the next generation of Arctic-system understanding where high resolution datasets and information will play a key role.

Acknowledgments. This work was supported by NSF Grant 0629279 and 0632133 and NASA Grant NNX08AI03G. The authors would like to thank Matthew Sturm for his insightful contributions to the direction of this research, and Skip Walker and Jed Kaplan for their land cover mapping discussions and advice. We would also like to thank the NASA Goddard Earth Sciences (GES) Data and Information Services Center (DISC) and Global Modeling and Assimilation Office (GMAO) for providing the MERRA datasets.

REFERENCES

- Aanes R., Sæther B.-E., Øritsland N. A., 2000: Fluctuations of an introduced population of Svalbard reindeer: the effects of density dependence and climatic variation. *Ecography*, **23**, 437-443.
- Adam, J. C., and D. P. Lettenmaier, 2003: Adjustment of global gridded precipitation for systematic bias. *J Geophys Res-Atmos*, **108**, 4257, doi:4210.1029/2002JD002499.
- Adam, J. C., A. F. Hamlet, and D. P. Lettenmaier, 2009: Implications of global climate change for snowmelt hydrology in the twenty-first century. *Hydrological Processes*, **23**, 962-972.
- Armstrong, R. L., and M. J. Brodzik, 2001: Validation of passive microwave snow algorithms. *Remote Sensing and Hydrology 2000. International Association of Hydrological Sciences Pub. No. 267*, M. Owe, K. Brubaker, J. Ritchie, and A. Rango, Eds., 87-92.
- Barnes, S. L., 1964: A technique for maximizing details in numerical weather map analysis. *J. Appl. Meteor.*, **3**, 396-409.
- Barnes, S. L., 1973: Mesoscale objective analysis using weighted time-series observations. NOAA Tech. Memo. ERL NSSL-62, National Severe Storms Laboratory, Norman, OK 73069, 60 pp. [NTIS COM-73-10781].
- Bartlett, M. G., D. S. Chapman, and R. N. Harris, 2005: Snow effect on North American ground temperatures, 1950-2002. *Journal of Geophysical Research-Earth Surface*, **110**, F03008, doi:03010.01029/02005/JF000293.
- Bhatt, U. S., D. A. Walker, M. K. Reynolds, J. C. Comiso, H. E. Epstein, G. S. Jia, R. Gens, J. E. Pinzon, C. J. Tucker, C. E. Tweedie, and P. J. Webber, 2010: Circumpolar Arctic tundra vegetation change is linked to sea ice decline. *Earth Interactions*, **14**, doi:10.1175/2010EI1315.1171.

- Bonsal, B. R., and B. Kochtubajda, 2009: An assessment of present and future climate in the Mackenzie Delta and the near-shore Beaufort Sea region of Canada. *Int J Climatol*, **29**, 1780-1795.
- Bosilovich, M., 2008: NASA's Modern Era Retrospective-analysis for Research and Applications: Integrating Earth Observations. *Earthzine*.
<http://www.earthzine.org/2008/09/26/nasas-modern-era-retrospective-analysis/>
- Bosilovich, M. G., J. Chen, F. R. Robertson, and R. F. Adler, 2008: Evaluation of global precipitation reanalyses. *J. Applied Meteorol. and Climatology*, **47**, 2279-2299.
- Bowling, L. C., J. W. Pomeroy, and D. P. Lettenmaier, 2004: Parameterization of blowing-snow sublimation in a macroscale hydrology model. *J. Hydrometeorology*, **5**, 745-762.
- Bromwich, D. H., Y.-H. Kuo, M. C. Serreze, J. E. Walsh, L. S. Bai, M. Barlage, K. M. Hines, and A. S. Slater, 2010: Arctic System Reanalysis: Call for community involvement. *EOS, Transactions, AGU*, **91**, 13-14.
- Brown, R. D., 2000: Northern hemisphere snow cover variability and change, 1915-97. *J. Climate*, **13**, 2339-2355.
- Brown, R. D., and P. W. Mote, 2009: The response of Northern Hemisphere snow cover to a changing climate. *J. Climate*, **22**, 2124-2145.
- Brown, R., C. Derksen, and L. Wang, 2007: Assessment of spring snow cover duration variability over northern Canada from satellite datasets. *Remote Sens Environ*, **111**, 367-381.
- Brown, R., C. Derksen, and L. Wang, 2010: A multi-data set analysis of variability and change in Arctic spring snow cover extent, 1967-2008. *J Geophys Res-Atmos*, **115**, D16111, doi:16110.11029/12010JD013975.

- Bruland, O., G. E. Liston, J. Vonk, and A. Killingtveit, 2004: Modelling the snow distribution at two High-Arctic sites at Svalbard, Norway, and at a Sub-Arctic site in Central Norway. *Nordic Hydrology*, **35**, 191-208.
- Bunn, A. G., and S. J. Goetz, 2006: Trends in satellite-observed circumpolar photosynthetic activity from 1982 to 2003: The influence of seasonality, cover type, and vegetation density. *Earth Interactions*, **10**, 1-19.
- CAVM Team, 2003: Circumpolar Arctic Vegetation Map. Scale 1:7,500,000. Conservation of Arctic Flora and Fauna (CAFF) Map No. 1. U.S. Fish and Wildlife Service, Anchorage, Alaska. ISBN: 0-9767525-0-6 • ISBN-13: 978-0-9767525-0-9
- Chapin, F. S., M. Sturm, M. C. Serreze, J. P. McFadden, J. R. Key, A. H. Lloyd, A. D. McGuire, T. S. Rupp, A. H. Lynch, J. P. Schimel, J. Beringer, W. L. Chapman, H. E. Epstein, E. S. Euskirchen, L. D. Hinzman, G. Jia, C. L. Ping, K. D. Tape, C. D. C. Thompson, D. A. Walker, and J. M. Welker, 2005: Role of land-surface changes in Arctic summer warming. *Science*, **310**, 657-660.
- Choi, G., D. A. Robinson, and S. Kang, 2010: Changing Northern Hemisphere snow seasons. *J. Climate*, **23**, 5305-5310.
- Clein, J., A. D. McGuire, E. S. Euskirchen, and M. Calef, 2007: The effects of different climate input datasets on simulated carbon dynamics in the Western Arctic. *Earth Interactions*, **11**, 1-24.
- de Beurs, K. M., and G. M. Henebry, 2010: A land surface phenology assessment of the northern polar regions using MODIS reflectance time series. *Can J Remote Sens*, **36**, S87-S110.
- Derksen, C., P. Toose, A. Rees, L. Wang, M. English, A. Walker, and M. Sturm, 2010: Development of a tundra-specific snow water equivalent retrieval algorithm for satellite

- passive microwave data. *Remote Sens Environ*, **114**, 1699-1709.
- Drobot, S., J. Maslanik, U. C. Herzfeld, C. Fowler, and W. L. Wu, 2006: Uncertainty in temperature and precipitation datasets over terrestrial regions of the Western Arctic. *Earth Interactions*, **10**, 1-17.
- Dye, D. G., 2002: Variability and trends in the annual snow-cover cycle in Northern Hemisphere land areas, 1972-2000. *Hydrological Processes*, **16**, 3065-3077.
- Euskirchen, E. S., A. D. McGuire, and F. S. Chapin, 2007: Energy feedbacks of northern high-latitude ecosystems to the climate system due to reduced snow cover during 20th century warming. *Global Change Biol*, **13**, 2425-2438.
- Euskirchen, E. S., A. D. McGuire, T. S. Rupp, F. S. Chapin, and J. E. Walsh, 2009: Projected changes in atmospheric heating due to changes in fire disturbance and the snow season in the western Arctic, 2003-2100. *J Geophys Res-Biogeophys*, **114**, G04022, doi:10.1029/2009JG001095.
- Finnis, J., J. J. Cassano, M. Holland, M. C. Serreze, and P. Uotila, 2009a: Synoptically forced hydroclimatology of major Arctic watersheds in general circulation models; Part 2: Eurasian watersheds. *Int J Climatol*, **29**, 1244-1261.
- Finnis, J., J. Cassano, M. Holland, M. Serreze, and P. Uotila, 2009b: Synoptically forced hydroclimatology of major Arctic watersheds in general circulation models; Part 1: the Mackenzie River Basin. *Int J Climatol*, **29**, 1226-1243.
- Frei, A., and D. A. Robinson, 1999: Northern Hemisphere snow extent: Regional variability 1972–1994. *Int. J. Climatol.*, **19**, 1535–1560.
- Gerland, S., A. H. H. Renner, F. Godtliessen, D. Divine, and T. B. Loynning, 2008: Decrease of sea ice thickness at Hopen, Barents Sea, during 1966-2007. *Geophysical Research*

Letters, **35** L06501, doi:06510.01029/02007GL032716.

Greene, E. M., G. E. Liston, and R. A. Pielke Sr., 1999: Simulation of above treeline snowdrift formation using a numerical snow-transport model. *Cold Regions Sci. Tech.*, **30**, 135-144.

Hasholt, B., G. E. Liston, and N. T. Knudsen, 2003: Snow distribution modelling in the Ammassalik Region, South East Greenland. *Nordic Hydrology*, **34**, 1-16.

Hiemstra, C. A., G. E. Liston, and W. A. Reiners, 2002: Snow redistribution by wind and interactions with vegetation at upper treeline in the Medicine Bow Mountains, Wyoming, USA. *Arctic, Antarctic, and Alpine Research*, **34**, 262-273.

Hiemstra, C. A., G. E. Liston, and W. A. Reiners, 2006: Observing, modelling, and validating snow redistribution by wind in a Wyoming upper treeline landscape. *Ecological Modelling*, **197**, 35-51.

Hines, K. M., D. H. Bromwich, L.-S. Bai, M. Barlage, and A. G. Slater, 2010: Development and testing of Polar WRF. Part III. Arctic Land. *Journal of Climate*, in press, doi: 10.1175/2010JCLI3460.1.

Hinzman, L. D., N. D. Bettez, W. R. Bolton, F. S. Chapin, M. B. Dyurgerov, C. L. Fastie, B. Griffith, R. D. Hollister, A. Hope, H. P. Huntington, A. M. Jensen, G. J. Jia, T. Jorgenson, D. L. Kane, D. R. Klein, G. Kofinas, A. H. Lynch, A. H. Lloyd, A. D. McGuire, F. E. Nelson, W. C. Oechel, T. E. Osterkamp, C. H. Racine, V. E. Romanovsky, R. S. Stone, D. A. Stow, M. Sturm, C. E. Tweedie, G. L. Vourlitis, M. D. Walker, D. A. Walker, P. J. Webber, J. M. Welker, K. Winker, and K. Yoshikawa, 2005: Evidence and implications of recent climate change in northern Alaska and other arctic regions. *Climatic Change*, **72**, 251-298.

Holland, M. M., M. C. Serreze, and J. Stroeve, 2010: The sea ice mass budget of the Arctic and

- its future change as simulated by coupled climate models. *Clim Dynam*, **34**, 185-200.
- Koch, S. E., M. DesJardins, P. J. Kocin, 1983: An interactive Barnes objective map analysis scheme for use with satellite and conventional data. *J. Clim. and Appl. Meteorol.*, **22**, 1487-1503.
- Liston, G. E., 1995: Local advection of momentum, heat, and moisture during the melt of patchy snow covers. *J. Applied Meteorol.*, **34**, 1705-1715.
- Liston, G. E., 2004: Representing subgrid snow cover heterogeneities in regional and global models. *J. Climate*, **17**, 1381-1397.
- Liston, G. E., and K. Elder, 2006a: A distributed snow-evolution modeling system (SnowModel). *J. Hydrometeorology*, **7**, 1259-1276.
- Liston, G. E., and K. Elder, 2006b: A meteorological distribution system for high-resolution terrestrial modeling (MicroMet). *J. Hydrometeorology*, **7**, 217-234.
- Liston, G. E., and D. K. Hall, 1995: An energy balance model of lake ice evolution. *J. Glaciol.*, **41**, 373-382.
- Liston, G. E., and C. A. Hiemstra, 2008: A simple data assimilation system for complex snow distributions (SnowAssim). *J. Hydrometeorology*, **9**, 989-1004.
- Liston, G. E., and C. A. Hiemstra, 2010: Representing grass and shrub-snow-atmosphere interactions in climate-system models. *J. Climate*, in press.
- Liston, G. E., and S. H. Mernild, 2010: A runoff routing model for the Greenland Ice Sheet (IceHydro). *J. Climate*, in review.
- Liston, G. E., and M. Sturm, 1998: A snow-transport model for complex terrain. *J. Glaciology*, **44**, 498-516.
- Liston, G. E., and M. Sturm, 2002: Winter precipitation patterns in arctic Alaska determined

- from a blowing-snow model and snow-depth observations. *J. Hydrometeor.*, **3**, 646-659.
- Liston, G. E., and M. Sturm, 2004: The role of winter sublimation in the Arctic moisture budget. *Nordic Hydrology*, **35**, 325-334.
- Liston, G. E., and M. Sturm, 2010: A global snow classification dataset for Earth system applications. In review.
- Liston, G. E., and J.-G. Winther, 2005: Antarctic surface and subsurface snow and ice melt fluxes. *J. Climate*, **18**, 1469-1481.
- Liston, G. E., J. -G. Winther, O. Bruland, H. Elvehøy, and K. Sand, 1999: Below-surface ice melt on the coastal Antarctic ice sheet. *J. Glaciol.*, **45**, 273-285.
- Liston, G. E., J. -G. Winther, O. Bruland, H. Elvehøy, K. Sand, and L. Karlöf, 2000: Snow and blue-ice distribution patterns on the coastal Antarctic ice sheet. *Antarctic Science*, **12**, 69-79.
- Liston, G. E., J. P. McFadden, M. Sturm, and R. A. Pielke, Sr., 2002: Modeled changes in arctic tundra snow, energy, and moisture fluxes due to increased shrubs. *Global Change Biology*, **8**, 17-32.
- Liston, G. E., R. B. Haehnel, M. Sturm, C. A. Hiemstra, S. Berezovskaya, and R. D. Tabler, 2007: Simulating complex snow distributions in windy environments using SnowTran-3D. *Journal of Glaciology*, **53**, 241-256.
- Liston, G. E., C. A. Hiemstra, K. Elder, and D. W. Cline, 2008: Meso-cell study area (MSA) snow distributions for the Cold Land Processes Experiment (CLPX). *J. Hydrometeorology*, **9**, 957-976.
- Lynch, A. H., A. G. Slater, and M. Serreze, 2001: The Alaskan Arctic frontal zone: forcing by orography, coastal contrast, and the boreal forest. *J. Climate*, **14**, 4351-4362.

- McCabe, G. J., and D. M. Wolock, 2010: Long-term variability in Northern Hemisphere snow cover and associations with warmer winters. *Climatic Change*, **99**, 141-153.
- McGuire, A. D., F. S. Chapin, J. E. Walsh, and C. Wirth, 2006: Integrated regional changes in arctic climate feedbacks: Implications for the global climate system. *Annu Rev Env Resour*, **31**, 61-91.
- McGuire, A. D., J. E. Walsh, J. S. Kimball, J. S. Clein, E. S. Euskirchen, S. Drobot, U. C. Herzfeld, J. Maslanik, R. B. Lammers, M. A. Rawlins, C. J. Vorosmarty, T. S. Rupp, W. Wu, and M. Calef, 2008: The western Arctic Linkage Experiment (WALE): Overview and synthesis. *Earth Interactions*, **12**, 1-13.
- McNamara, J. P., D. L. Kane, and L. D. Hinzman, 1998: An analysis of streamflow hydrology in the Kuparuk River Basin, Arctic Alaska: a nested watershed approach. *J. Hydrol.*, **206**, 39-57.
- Mernild, S. H., and G. E. Liston, 2010: The influence of air temperature inversions on snowmelt and glacier mass-balance simulations, Ammassalik Island, SE Greenland. *J. Applied Meteorology and Climatology*, **49**, 47-67.
- Mernild, S. H., G. E. Liston, B. Hasholt, and N. T. Knudsen, 2006: Snow-distribution and melt modeling for Mittivakkat Glacier, Ammassalik Island, Southeast Greenland. *J. Hydrometeorology*, **7**, 808-824.
- Mernild, S., H., B. Hasholt, and G. E. Liston, 2008: Climatic control on river discharge simulations, Zackenberg River drainage basin, northeast Greenland. *Hydrological Processes*, **22**, 1932-1948.
- Mernild, S. H., G. E. Liston, C. A. Hiemstra, K. Steffen, E. Hanna, and J. H. Christensen, 2009: Greenland Ice Sheet surface mass-balance modelling and freshwater flux for 2007, and in

- a 1995–2007 perspective. *Hydrological Processes*, DOI: 10.1002/hyp.7354.
- Mernild, S. H., G. E. Liston, C. A. Hiemstra, and J. H. Christensen, 2010: Greenland Ice Sheet surface mass-balance modeling in a 131-year perspective, 1950-2080. *J. Hydrometeorology*, **11**, 3-25, DOI:10.1175/2009JHM1140.1.
- New, M., M. Todd, M. Hulme, and P. Jones, 2001: Precipitation measurements and trends in the twentieth century. *Int J Climatol*, **21**, 1899-1922.
- Overland, J. E., M. C. Spillane, D. B. Percival, M. Y. Wang, and H. O. Mofjeld, 2004: Seasonal and regional variation of pan-Arctic surface air temperature over the instrumental record. *Journal of Climate*, **17**, 3263-3282.
- Pohl, S., P. Marsh, and B. R. Bonsal, 2007: Modeling the impact of climate change on runoff and annual water balance of an Arctic headwater basin. *Arctic*, **60**, 173-186.
- Post, E., M. C. Forchhammer, M. S. Bret-Harte, T. V. Callaghan, T. R. Christensen, B. Elberling, A. D. Fox, O. Gilg, D. S. Hik, T. T. Hoye, R. A. Ims, E. Jeppesen, D. R. Klein, J. Madsen, A. D. McGuire, S. Rysgaard, D. E. Schindler, I. Stirling, M. P. Tamstorf, N. J. C. Tyler, R. van der Wal, J. Welker, P. A. Wookey, N. M. Schmidt, and P. Aastrup, 2009: Ecological dynamics across the Arctic associated with recent climate change. *Science*, **325**, 1355-1358.
- Prasad, R., D. G. Tarboton, G. E. Liston, C. H. Luce, and M. S. Seyfried, 2001: Testing a blowing snow model against distributed snow measurements at Upper Sheep Creek, Idaho, USA. *Water Resour. Res.*, **37**, 1341-1357.
- Putkonen, J., and G. H. Roe, 2003: Rain-on-snow events, soil temperatures, and the sensitivity of ungulates to climate change. *Geophys. Res. Lett.*, **30**, doi: 10.1029/2002GL016326.
- Putkonen, J., T. C. Grenfell, K. Rennert, C. Bitz, P. Jacobson, and D. Russell, 2009: Rain on

- snow: little understood killer in the North. *Eos Trans., AGU*, **90**,
doi:10.1029/2009EO260002.
- Räisänen, J., 2008: Warmer climate: less or more snow? *Clim Dynam*, **30**, 307-319.
- Rennert, K. J., G. Roe, J. Putkonen, C. M. Bitz, 2009: Soil thermal and ecological impacts of rain on snow events in the circumpolar Arctic. *J. Climate*, **22**, 2302-2315.
- Roberts, A., and coauthors, 2010: A Science Plan for Regional Arctic System Modeling, A report to the National Science Foundation from the International Arctic Science Community. International Arctic Research Center Technical Papers 10-0001. International Arctic Research Center, University of Alaska Fairbanks.
- Romanovsky, V. E., S. L. Smith, and H. H. Christiansen, 2010: Permafrost thermal state in the Polar Northern Hemisphere during the International Polar Year 2007-2009: a synthesis. *Permafrost and Periglacial Processes*, **21**, 106-116.
- Serreze, M. C., and R. G. Barry, 2005: *The Arctic Climate System*. Cambridge University Press, 385 pp.
- Serreze, M. C., and J. A. Francis, 2006: The arctic amplification debate. *Climatic Change*, **76**, 241-264.
- Serreze, M. C., J. E. Walsh, F. S. Chapin, T. Osterkamp, M. Dyurgerov, V. Romanovsky, W. C. Oechel, J. Morison, T. Zhang, and R. G. Barry, 2000: Observational evidence of recent change in the northern high-latitude environment. *Climatic Change*, **46**, 159-207.
- Serreze, M. C., A. P. Barrett, and F. Lo, 2005: Northern high-latitude precipitation as depicted by atmospheric reanalyses and satellite retrievals. *Mon Weather Rev*, **133**, 3407-3430.
- Shukla, J., T. N. Palmer, R. Hagedorn, B. Hoskins, J. Kinter, J. Marotzke, M. Miller, J. Slingo, 2010: Toward a new generation of world climate research and computing facilities.

- Bulletin American Meteorological Society*, **91**, 1407-1412, doi:
10.1175/2010BAMS2900.1.
- Shulski, M., and G. Wendler, 2007: *The climate of Alaska*. University of Alaska Press, 216 pp.
- Slater, A. G., T. J. Bohn, J. L. McCreight, M. C. Serreze, and D. P. Lettenmaier, 2007: A multimodel simulation of pan-Arctic hydrology. *J Geophys Res-Bioge*, **112**, G04S45, doi:10.1029/2006JG000303.
- Solomon, S., D. Qin, M. Manning, Z. Chen, M. Marquis, K. B. Averyt, M. Tignor, and H. L. Miller, Eds., 2007: *Contribution of Working Group I to the Fourth Assessment Report of the Intergovernmental Panel on Climate Change*. Cambridge University Press 996 pp.
- Stone, R. S., E. G. Dutton, J. M. Harris, and D. Longenecker, 2002: Earlier spring snowmelt in northern Alaska as an indicator of climate change. *J Geophys Res-Atmos*, **107**, D10, 4089, doi: 4010.1029/2000JD000286.
- Stroeve, J., M. M. Holland, W. Meier, T. Scambos, and M. Serreze, 2007: Arctic sea ice decline: Faster than forecast. *Geophysical Research Letters*, **34**, L09501, doi:09510.01029/02007GL029703.
- Sturm, M., J. Holmgren, and G. E. Liston, 1995: A seasonal snow cover classification system for local to global applications. *J. Climate*, **8**, 1261-1283.
- Sturm, M., B. Taras, G. E. Liston, C. Derksen, T. Jonas, and J. Lea, 2010: Estimating snow water equivalent using snow depth data and climate classes. *J. Hydrometeorology*, in press, doi: 10.1175/2010JHM1202.1.
- Taras, B., M. Sturm, and G. E. Liston, 2002: Snow-ground interface temperatures in the Kuparuk River Basin, arctic Alaska: Measurements and model. *J. Hydrometeorology*, **3**, 377-394.
- Turner, J., and J. Overland, 2009: Contrasting climate change in the two polar regions. *Polar*

- Research*, **28**, 146-164.
- Turner, J., J. E. Overland, and J. E. Walsh, 2007: An Arctic and Antarctic perspective on recent climate change. *Int J Climatol*, **27**, 277-293.
- Verbyla, D., 2008: The greening and browning of Alaska based on 1982-2003 satellite data. *Global Ecology and Biogeography*, **17**, 547-555.
- Walsh, J. E., W. L. Chapman, V. Romanovsky, J. H. Christensen, and M. Stendel, 2008: Global Climate Model Performance over Alaska and Greenland. *Journal of Climate*, **21**, 6156-6174.
- Wendler, G., and M. Shulski, 2009: A Century of Climate Change for Fairbanks, Alaska. *Arctic*, **62**, 295-300.
- White, D., L. Hinzman, L. Alessa, J. Cassano, M. Chambers, K. Falkner, J. Francis, W. J. Gutowski, M. Holland, R. M. Holmes, H. Huntington, D. Kane, A. Kliskey, C. Lee, J. McClelland, B. Peterson, T. S. Rupp, F. Straneo, M. Steele, R. Woodgate, D. Yang, K. Yoshikawa, and T. Zhang, 2007: The arctic freshwater system: Changes and impacts. *J Geophys Res-Bioge*, **112**, G04S54, doi:10.1029/2006JG00035.
- Wulder, M. A., T. A. Nelson, C. Derksen, and D. Seemann, 2007: Snow cover variability across central Canada (1978-2002) derived from satellite passive microwave data. *Climatic Change*, **82**, 113-130.
- Yang, D., D. Robinson, Y. Zhao, T. Estilow, and B. Ye, 2003: Streamflow response to seasonal snowcover extent changes in large Siberian watersheds. *Journal of Geophysical Research-Atmospheres*, **108**(D18), 4578, doi: 10.1029/2002JD003149.
- Yang, D., B. Ye, and A. Shiklomanov, 2004: Streamflow characteristics and changes over the Ob river watershed in Siberia. *J. Hydrometeorology*, **5**, 69-84.

- Yang, D. Q., D. Kane, Z. P. Zhang, D. Legates, and B. Goodison, 2005: Bias corrections of long-term (1973-2004) daily precipitation data over the northern regions. *Geophysical Research Letters*, **32**, L19501 doi:19510.11029/12005GL024057.
- Zhang, T. J., 2005: Influence of the seasonal snow cover on the ground thermal regime: An overview. *Reviews of Geophysics*, **43**, RG4002, doi:4010.1029/2004RG000157.
- Zhao, H. X., and R. Fernandes, 2009: Daily snow cover estimation from Advanced Very High Resolution Radiometer Polar Pathfinder data over Northern Hemisphere land surfaces during 1982-2004. *J Geophys Res-Atmos*, **114**, D05113, doi:05110.01029/02008JD011272.

FIGURE CAPTIONS

Fig. 1. (a) 7250-km by 7250-km simulation domain, color shades are topography (color increment is not linear), and MERRA atmospheric forcing (black dots; to improve clarity, only every other grid point was plotted in x and y, i.e., 25% of the grid points are shown). (b) Land cover distribution. To improve clarity, some classes have been lumped together into a single color (e.g., in SnowModel there are 3 Arctic shrub types in this domain).

Fig. 2. (a) 30-year average, 10-m air temperature, when snow was on the ground ($^{\circ}\text{C}$). (b) Trend in 10-m air temperature ($^{\circ}\text{C decade}^{-1}$) when snow was on the ground. (c) Area- and yearly-averaged 10-m air temperature, when snow was on the ground, for the 250-km by 250-km Alaska box in (a) and (b). (d) Area- and yearly-averaged 10-m air temperature, when snow was on the ground, for the 250-km by 250-km Canada box in (a) and (b).

Fig. 3. Same as Fig. 2, but for total annual snow precipitation in water-equivalent units. (a) cm, (b) cm decade^{-1} .

Fig. 4. Same as Fig. 2, but for snow duration during the core snow season. (a) days, (b) days decade^{-1} . The core snow season is defined to be the longest period of continuous snow cover in each year [e.g., the blue shading in the (a) inset].

Fig. 5. Same as Fig. 2, but for the onset of the core snow season. (a) date, (b) days decade^{-1} .

Fig. 6. Same as Fig. 2, but for the end of the core snow season. (a) date, (b) days decade⁻¹.

Fig. 7. Same as Fig. 2, but for the maximum seasonal snow-water-equivalent depth during each year. (a) cm, (b) cm decade⁻¹.

Fig. 8. Same as Fig. 2, but for the average snow density. (a) kg m⁻³, (b) kg m⁻³ decade⁻¹.

Fig. 9. Same as Fig. 2, but for the total snow sublimation during each year. (a) mm, (b) mm decade⁻¹.

Fig. 10. Same as Fig. 2, but for the number of rain-on-snow days during each year. (a) days, (b) days decade⁻¹.

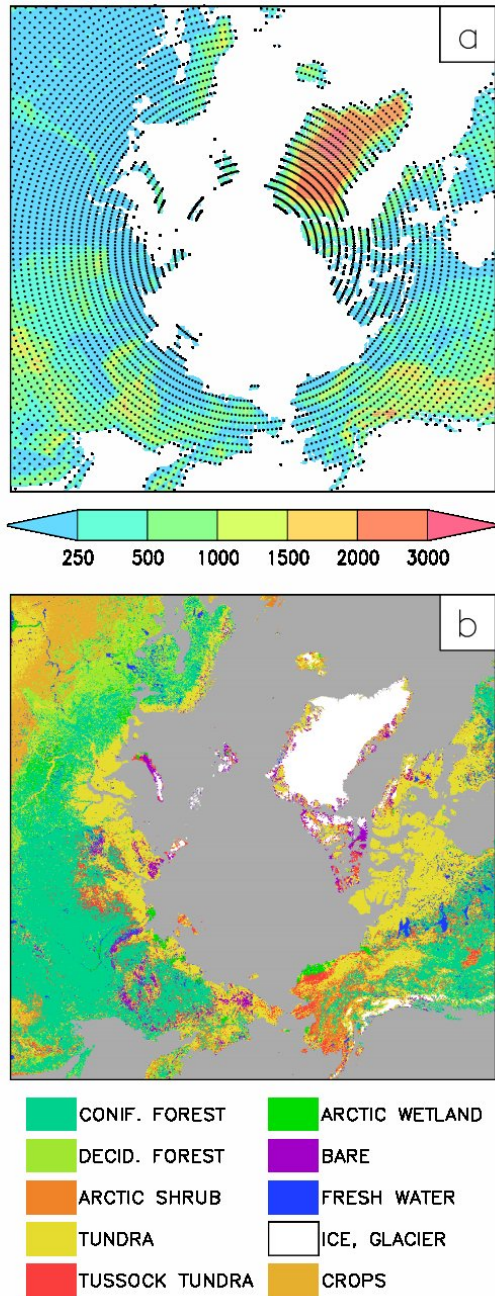


Fig. 1. (a) 7250-km by 7250-km simulation domain, color shades are topography (color increment is not linear), and MERRA atmospheric forcing (black dots; to improve clarity, only every other grid point was plotted in x and y, i.e., 25% of the grid points are shown). (b) Land cover distribution. To improve clarity, some classes have been lumped together into a single color (e.g., in SnowModel there are 3 Arctic shrub types in this domain).

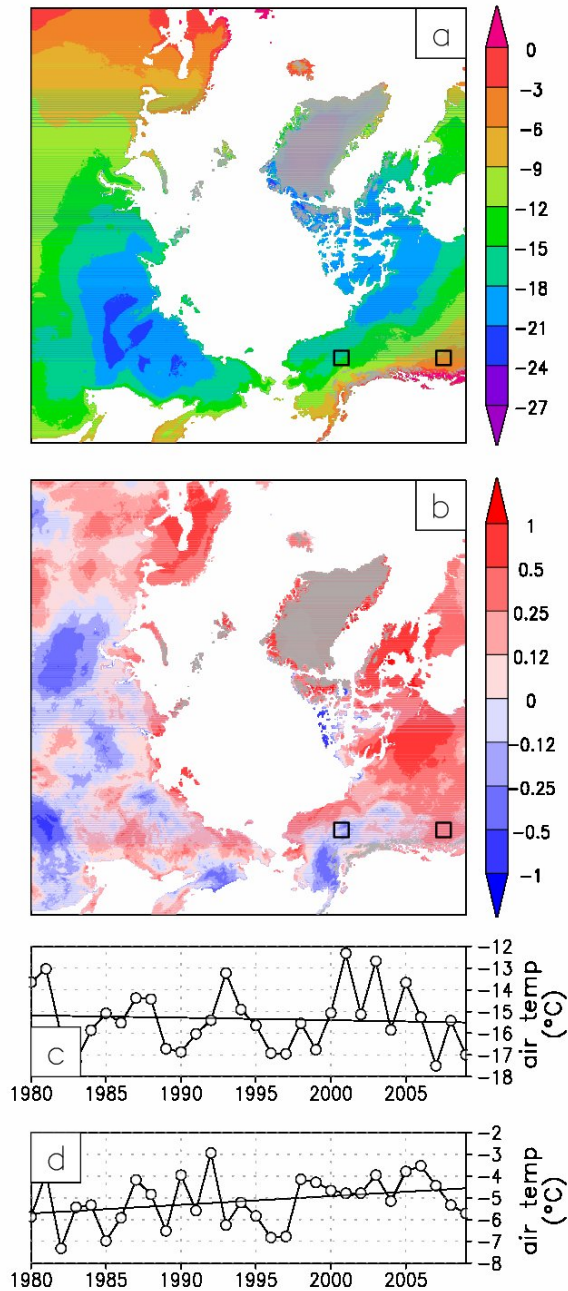


Fig. 2. (a) 30-year average, 10-m air temperature, when snow was on the ground (°C). (b) Trend in 10-m air temperature (°C decade⁻¹) when snow was on the ground. (c) Area- and yearly-averaged 10-m air temperature, when snow was on the ground, for the 250-km by 250-km Alaska box in (a) and (b). (d) Area- and yearly-averaged 10-m air temperature, when snow was on the ground, for the 250-km by 250-km Canada box in (a) and (b).

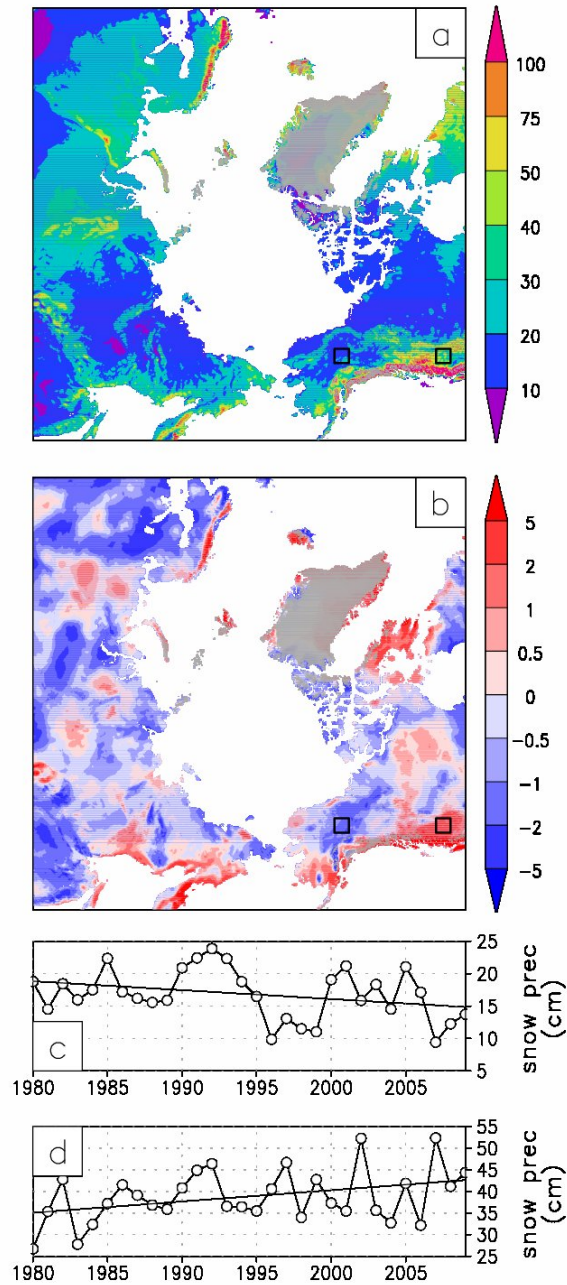


Fig. 3. Same as Fig. 2, but for total annual snow precipitation in water-equivalent units.

(a) cm, (b) cm decade⁻¹.

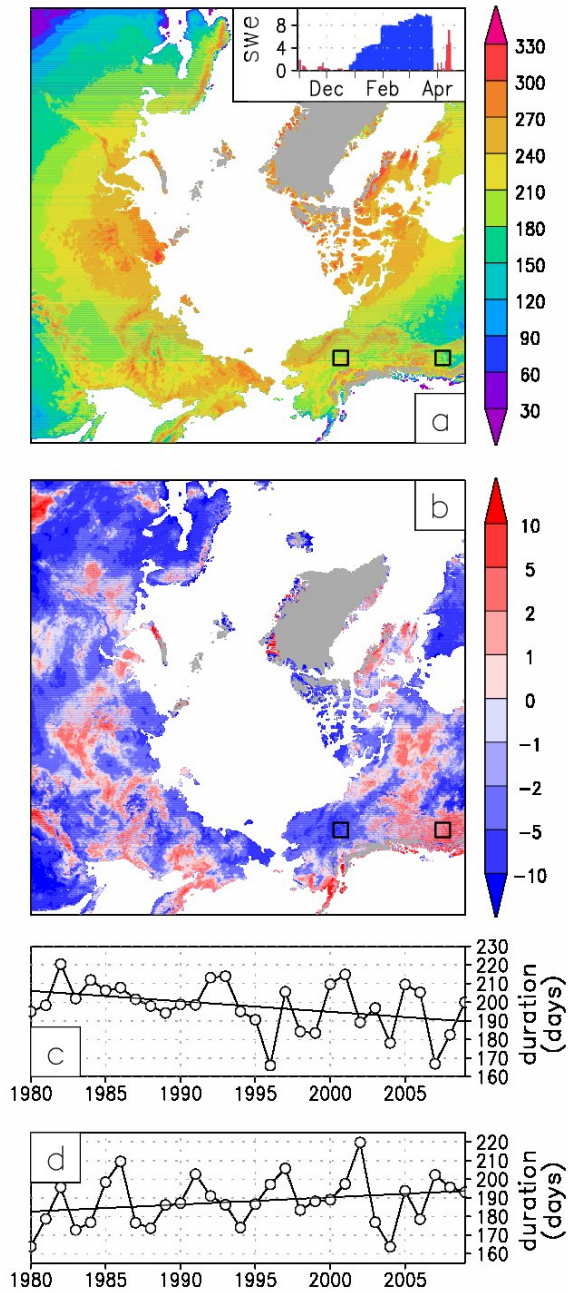


Fig. 4. Same as Fig. 2, but for snow duration during the core snow season. (a) days, (b) days decade⁻¹. The core snow season is defined to be the longest period of continuous snow cover in each year [e.g., the blue shading in the (a) inset].

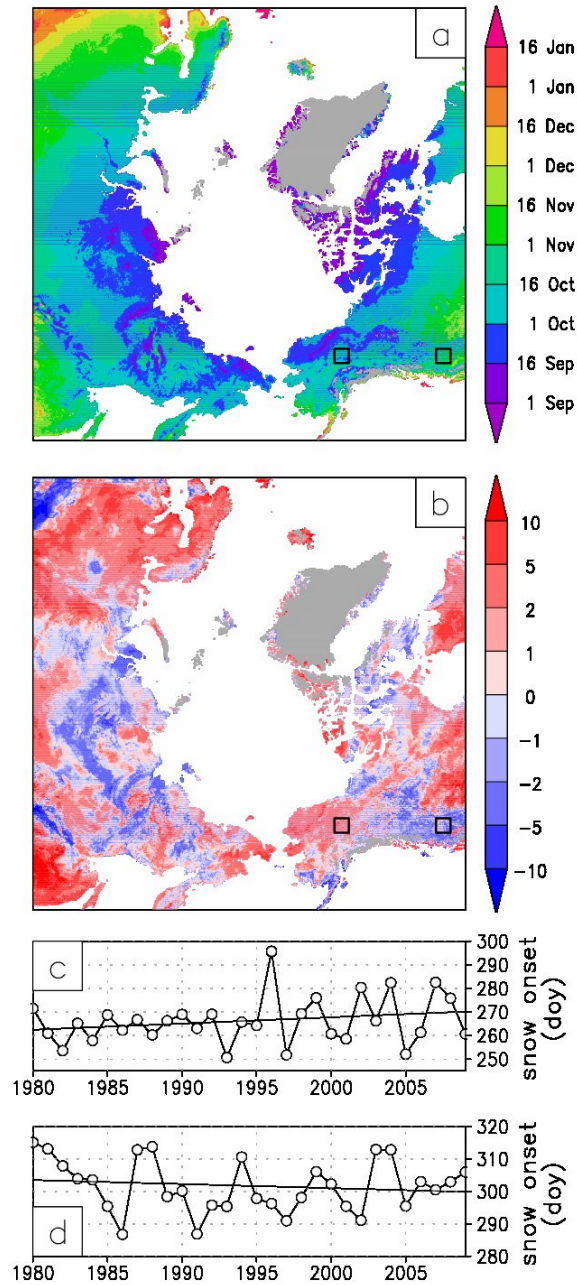


Fig. 5. Same as Fig. 2, but for the onset of the core snow season. (a) date, (b) days decade⁻¹.

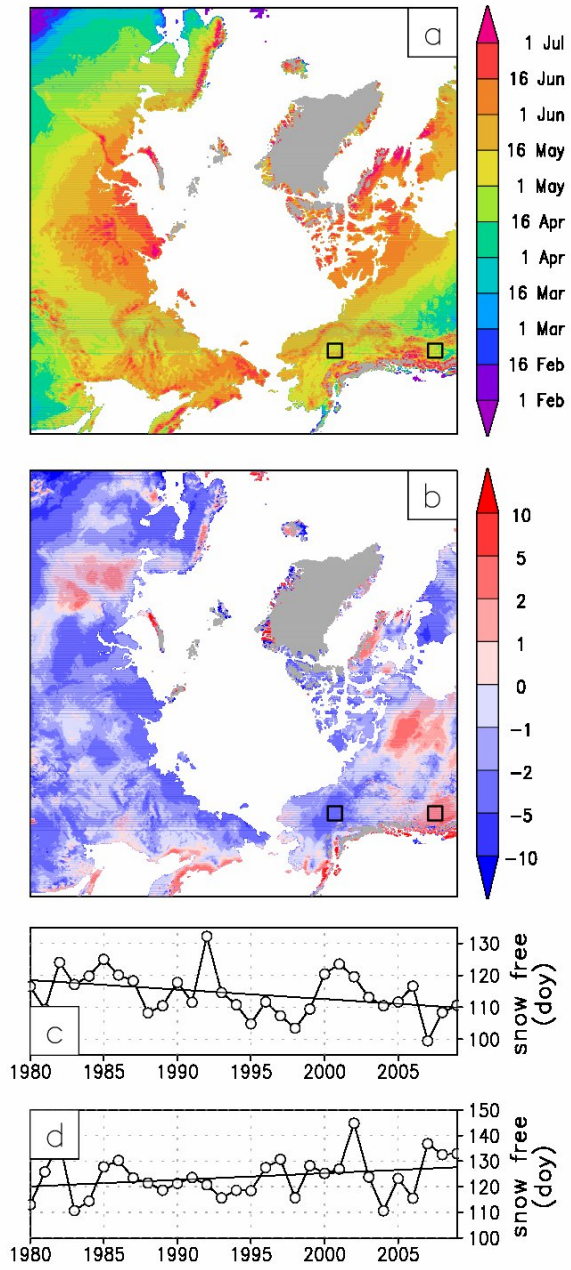


Fig. 6. Same as Fig. 2, but for the end of the core snow season. (a) date, (b) days decade⁻¹.

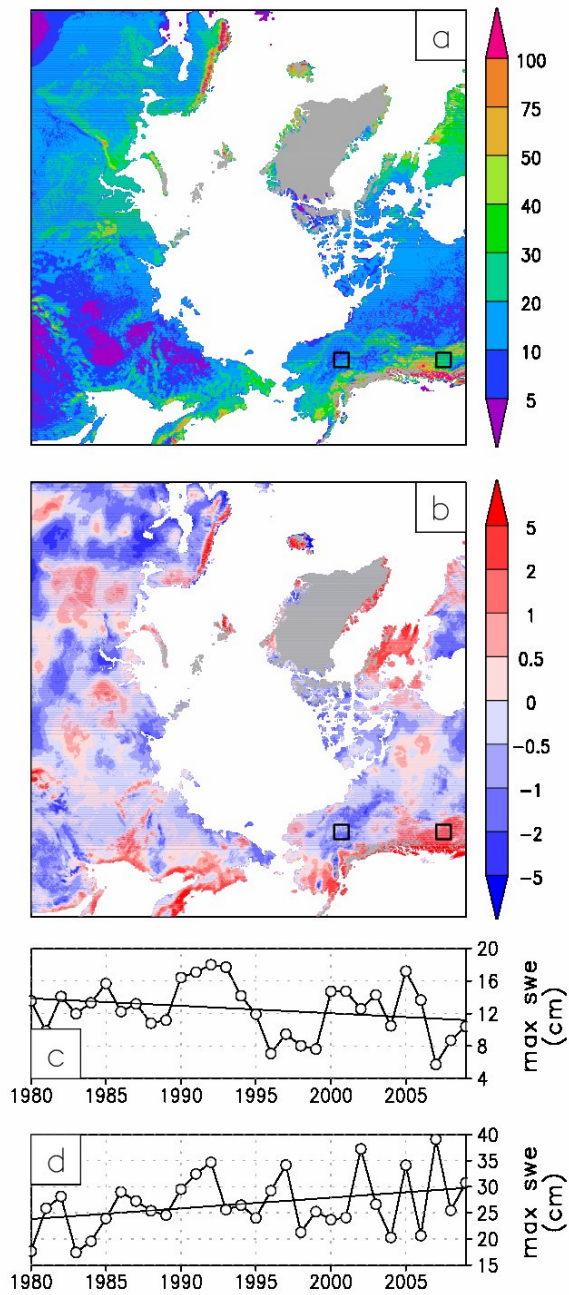


Fig. 7. Same as Fig. 2, but for the maximum seasonal snow-water-equivalent depth during each year. (a) cm, (b) cm decade^{-1} .

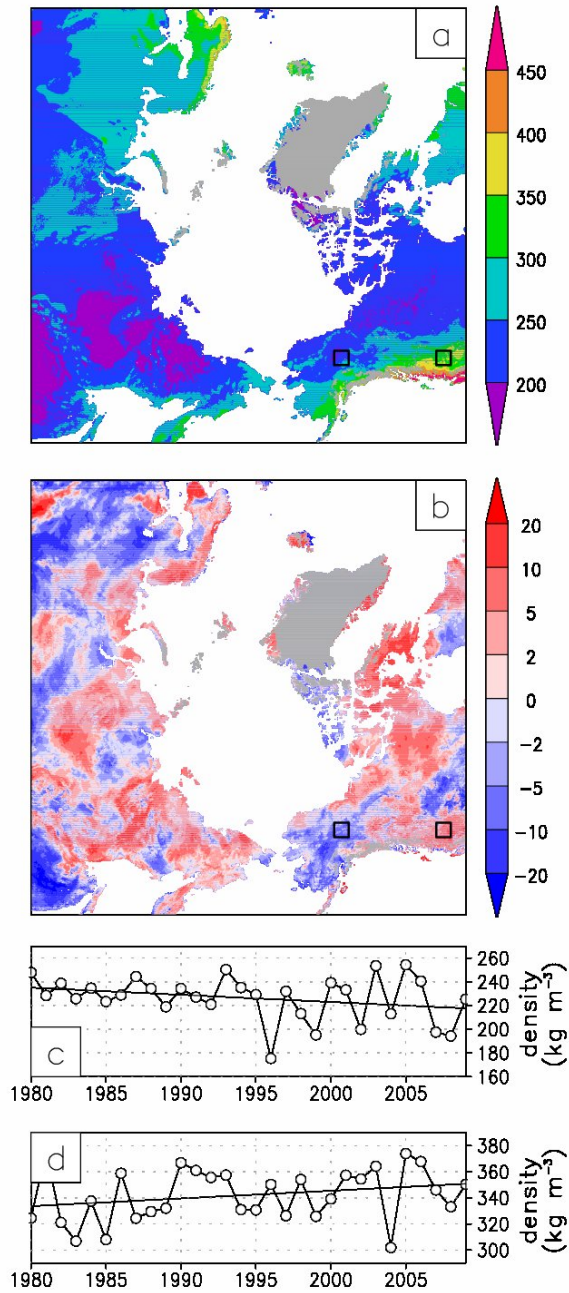


Fig. 8. Same as Fig. 2, but for the average snow density. (a) kg m^{-3} , (b) $\text{kg m}^{-3} \text{ decade}^{-1}$.

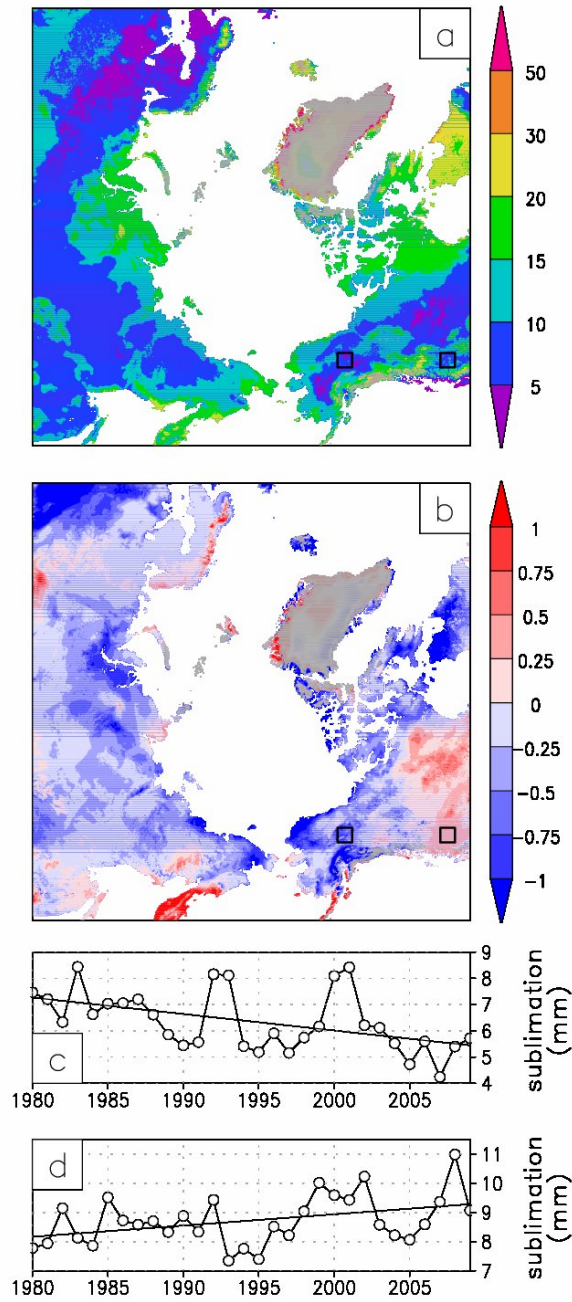


Fig. 9. Same as Fig. 2, but for the total snow sublimation during each year. (a) mm, (b) mm decade⁻¹.

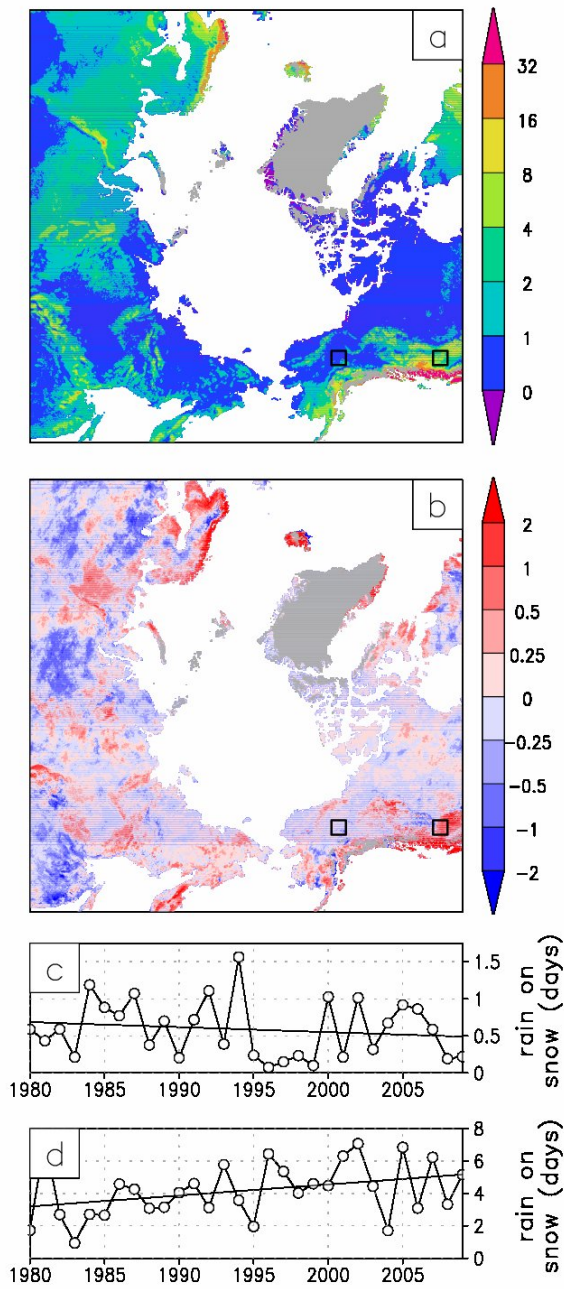


Fig. 10. Same as Fig. 2, but for the number of rain-on-snow days during each year. (a) days, (b) days decade⁻¹.

Table 1. Domain average, and minimum and maximum regional, trends of snow-related variables. A region was defined to be a 250-km by 250-km area that was free of ice or ocean grid cells [see boxes in panels (a) and (b) of Figs. 2-10 for examples]. Statistical significance was calculated for the trends, and also shown are the land fractions exhibiting positive and negative trends.

Variable	Trend Units	Domain Average Trend	Minimum Regional Trend	Maximum Regional Trend	Positive Trend Area (%)	Negative Trend Area (%)
Air temperature (with snow on the ground)	°C decade ⁻¹	0.17 ^a	-0.55 ^b	0.78 ^c	73	27
Air temperature (with and without snow)	°C decade ⁻¹	0.38 ^c	-0.04	0.78 ^c	99	1
Annual total snow precipitation	cm decade ⁻¹	-0.02	-3.03 ^c	8.00 ^c	36	64
Days in core snow season	days decade ⁻¹	-2.57 ^c	-17.01 ^c	8.11 ^a	25	75
Total snow days	days decade ⁻¹	-2.49 ^c	-17.21 ^c	7.19	24	76
Core snow season snow-onset date	days decade ⁻¹	1.29 ^c	-10.79 ^c	14.09 ^c	65	35
Core snow season snow-free date	days decade ⁻¹	-1.28 ^c	-9.89 ^a	3.74 ^b	20	80
Maximum seasonal snow	cm decade ⁻¹	-0.07	-2.50 ^c	5.70 ^c	39	61

water equivalent						
Average seasonal	kg m ⁻³	0.29	-20.98 ^c	15.43 ^c	54	46
snow density	decade ⁻¹					
Annual total snow	mm decade ⁻¹	-0.22	-1.87 ^c	1.41 ^b	23	77
sublimation						
Rain on snow	days decade ⁻¹	0.03	-0.96 ^c	1.50 ^c	48	52

^a Significant at the 90% confidence level.

^b Significant at the 95% confidence level.

^c Significant at the 99% confidence level.